Title
Intra- and Extra-articular Features of Temporomandibular Joint Ankylosis in the Cat (Felis catus)

Authors
Zavodovskaya, R
Vapniarsky, N
Garcia, T
et al.

Publication Date
2020-02-01

DOI
10.1016/j.jcpa.2019.12.006

Peer reviewed

J. Comp. Path. 2020, Vol. 175, 39–48

Available online at www.sciencedirect.com

ScienceDirect

ELSEVIER

www.elsevier.com/locate/jcpa

SPONTANEOUSLY ARISING DISEASE

Intra- and Extra-articular Features of Temporomandibular Joint Ankylosis in the Cat (*Felis catus*)

R. Zavodovskaya[*], N. Vapniarsky[†], T. Garcia[‡], F. J. M. Verstraete[§], D. C. Hatcher[§] and B. Arzi[§]

[*] *California Animal Health and Food Safety Laboratory System,* [†] *Department of Pathology, Microbiology and Immunology,* [‡] *Department of Anatomy, Physiology and Cell Biology and* [§] *Department of Surgical and Radiological Sciences, School of Veterinary Medicine, University of California, Davis, California, USA*

Summary

Temporomandibular joint (TMJ) ankylosis is an uncommon clinical entity in human and veterinary medicine. However, the condition is severely debilitating and is life-limiting if not treated. This study sought to characterize the intra- and extra-articular features of naturally occurring TMJ ankylosis in cats. TMJs from client-owned cats ($n = 5$) that underwent bilateral TMJ gap arthroplasty were examined and compared with TMJs from healthy, age-matched feline cadavers ($n = 2$) by cone-beam computed tomography (CBCT), micro-computed tomography (μCT) and histologically. Features of bilateral intra- and extra-articular ankylosis compounded by degenerative joint lesions were identified radiographically and histologically in all affected cats. Features of TMJ 'true' ankylosis included variable intracapsular fibro-osseous bridging, degeneration of the disc and the articular surfaces, narrowing of the joint space and flattening of the condylar process of the mandible. Extra-articular features of TMJ ankylosis included periarticular bone formation and fibro-osseous bridging between the mandible, zygomatic arch and coronoid process. In addition, subchondral bone loss or sclerosis, irregular and altered joint contours and irregularly increased density of the medullary bone characterized the degenerative changes of the osseous components of the TMJ. Complex radiological and histological features of both ankylosis and pseudoankylosis were identified that clinically manifested in complete inability to open the mouth.

Keywords: ankylosis; cat; computed tomography; temporomandibular joint

Introduction

Temporomandibular joint (TMJ) ankylosis is a rare, debilitating disease across species that manifests as partial or complete loss of movement of the mandible (Meomartino *et al.*, 1999; Gatineau *et al.*, 2008; Arzi *et al.*, 2013; Strøm *et al.*, 2016). Affected cats are typically presented with progressive inability to open the mouth (Maas and Theyse, 2007; Strøm *et al.*, 2016). Immobilization of the TMJ(s) has significant, adverse consequences for essential survival functions such as eating, drinking and panting as well as on grooming and vocalization. Additional implications of ankylosis include malocclusion and dental diseases such as periodontitis and mucosal ulceration. Historical classification of TMJ ankylosis is divided into intra-articular (true ankylosis) and extra-articular (false or pseudoankylosis) (Miller *et al.*, 1975; Maas and Theyse, 2007; Gatineau *et al.*, 2008; Strøm *et al.*, 2016).

Corresponding author: B. Arzi (e-mail: barzi@ucdavis.edu).

0021-9975/$ - see front matter
https://doi.org/10.1016/j.jcpa.2019.12.006

The TM is formed through the articulation of the condylar process of the mandible with the mandibular fossa of the squamous part of the temporal bone (Nickel *et al.*, 1986; Evans and de Lahunta, 2013). The TMJ articular disc divides the joint into two non-communicating compartments, and together with the lateral ligament and the joint capsule, comprises the soft tissue components of the TMJ. The TMJ of carnivores is categorized as a synovial, hinge-like joint (Evans and de Lahunta, 2013; Lin *et al.*, 2018; Arzi, 2020). The paired TMJs move synchronously and govern the degree of mouth opening. Likewise, pathological processes affecting the TMJ typically affect the degree and comfort of mouth opening. In addition, a group of paired masticatory muscles is responsible for closing and opening of the mouth, with minimal mandibular lateral movement in dogs (i.e. laterotrusion) and no lateral movement in cats (Arzi and Staszyk, 2019; Arzi *et al.*, 2019; Arzi, 2020). Compared with man, translation (i.e. rostrocaudal sliding movement) of the TMJs is minimal in carnivores (Lin *et al.*, 2018; Arzi *et al.*, 2019; Arzi, 2020). The majority of the masticatory muscles function to close the mouth, including the masseter, temporal and medial and lateral pterygoid muscles. The digastricus muscle is considered to be the only muscle that opens the mouth (Evans and de Lahunta, 2013).

Pathological stiffening or immobilization of a joint defines ankylosis (Neville *et al.*, 2002). Pathological production of fibrous, osseous or fibro-osseous tissue between the mandibles and the skull impedes the joint movement to various degrees. In true ankylosis, intracapsular bridging disrupts the two joint components enclosed by the joint capsule, including the fibrocartilaginous articular surfaces and the disc (Neville *et al.*, 2002). In contrast, intracapsular structures may remain intact in pseudoankylosis (Miller *et al.*, 1975; Maas and Theyse, 2007; Gatineau *et al.*, 2008; Strøm *et al.*, 2016). Bridging configuration between the mandible and the temporal, maxillary or zygomatic bone, or the base of the skull, varies in the pseudoankylosis. Ankylosis results from a bilateral or unilateral fusion of the TMJ constricting the mouth in a closed position (Petrikowski, 2016; Strøm *et al.*, 2016; Arzi, 2020).

Maxillofacial trauma due to falling or a vehicular injury are the predominant aetiologies of TMJ damage with progression to ankylosis in cats (Meomartino *et al.*, 1999; Maas and Theyse, 2007; Arzi *et al.*, 2013). Other causes are rare and include neoplasia (Maas and Theyse, 2007; Cetinkaya, 2012), localized or systemic inflammation and infection, and congenital malformations. Rheumatoid disorders are implicated in TMJ ankylosis in man (Sidebottom and Salha, 2013). The degree of mandibular deformation and malocclusion depends on the underlying cause of ankylosis and the age of the affected individual (Hennet and Harvey, 1992; Strøm *et al.*, 2016). Due to continuous and synchronized growth of the craniofacial bones, deformation may include the mandible and other bones of the skull in skeletally immature patients, resulting in deformation of the skull and facial disfigurement (Maas and Theyse, 2007; Movahed and Mercuri, 2015). However, the underlying mechanism of the maladaptive healing process through ankylosis following TMJ trauma remains elusive.

Diagnosis of TMJ disorders and, specifically, ankylosis or pseudoankylosis, relies on adequate diagnostic imaging (Bar-Am *et al.*, 2008; Arzi *et al.*, 2013; Cissell *et al.*, 2020). Computed tomography (CT) and cone-beam computed tomography (CBCT) are regarded as the gold-standard techniques for the diagnosis of TMJ disorders (Bar-Am *et al.*, 2008; Cissell *et al.*, 2020). Other advanced diagnostic techniques such as magnetic resonance imaging (MRI) may be used to detect soft tissues changes associated with TMJ disorders (Yuan *et al.*, 2015; Cissell *et al.*, 2020). Clinically, decreased mandibular range of motion, changes in the facial bone and muscle symmetry, malocclusion and sensitivity to palpation of TMJs during physical examination, together with medical history, may be suggestive of TMJ ankylosis or pseudoankylosis (Arzi, 2020).

In order to understand better the features of TMJ ankylosis in cats and its implications for decision-making for surgical planning, this study aimed to characterize the intra-articular and extra-articular features of the disorder through CBCT, micro- (μ) CT and histology. We hypothesized that ankylosis of the TMJ has several facets of bone and fibrous unions with the surrounding bones and that degenerative changes would be identified radiographically and histologically within fused joints.

Materials and Methods

Specimens

Ten TMJs from five client-owned cats that were presented to the Dentistry and Oral Surgery Service at the William R. Pritchard, Veterinary Medical Teaching Hospital, University of California, Davis, California, USA, for bilateral TMJ ankylosis were obtained during surgery. The cats were between the ages of 5 and 18 months (mean 9.6 months) and of body weight 2.8–4.2 kg (mean 3.5 kg) and all experienced severe restriction in mouth-opening, requiring surgical intervention. Two cats had a history of craniofacial trauma with evidence of healing fractures and three cats had unknown history. All cats underwent bilateral surgical correction of the ankylosis using a gap arthroplasty method as previously described (Arzi, 2020). The TMJ specimens obtained during gap arthroplasty were preserved in 10% neutral buffered formalin. For controls, four healthy TMJs from two age-matched domestic cats (aged 12–24 months), that were humanely destroyed for reasons not related to this study, were removed by gap arthroplasty in a similar fashion as in the affected cats and preserved in 10% neutral buffered formalin.

Cone-Beam Computed Tomography

Prior to gap arthroplasty surgery, the anatomical and structural features of the TMJs were evaluated by CBCT (NewTom 5G CBCT, NewTom, Verona, Italy). The field of view was 15 × 12 cm, and serial slices of the skull were obtained with a scan time of 18 s, which resulted in a voxel size (slice thickness) of 150 μm. For CBCT comparison, the two control cadaver heads were scanned with identical CBCT settings. The images were evaluated with Invivo 5 software (Anatomage, San Jose, California, USA) by an experienced TMJ radiologist (DH) and two experienced board-certified veterinary dentists and oral surgeons (BA and FV).

Micro-computed Tomography

Formalin-fixed TMJ specimens, including the entire joint and associated structures of the coronoid process and temporal and zygomatic bones, were scanned using μCT (μCT 35, Scanco Medical, Bassersdorf, Switzerland). For scanning, the specimens were encased within 10% formalin-soaked foam in order to preserve constant moisture content and placed in a 3.5 cm diameter non-attenuating plastic tube. The scanning parameters were 55 kVp 145 μA, integration 400 msec, averages of four exposures per projection, 1,000 projections per 180° with a 0.5 mm aluminum filter and 15 μm voxel size. Image noise was reduced using a low-pass Gaussian filter ($\sigma = 1$, support $= 2$). Digital images were reconstructed to maintain the anatomical planes of the TMJs.

Histology

Formalin-fixed TMJ specimens were decalcified in 10% formic acid for 3–4 weeks following μCT scanning. Decalcified specimens were bisected parasagittally through the centre of the TMJs, processed routinely and embedded in paraffin wax. Sections (5 μm) were stained with haematoxylin and eosin (HE) according to standard protocol (Carson, 1997). Additional sections were stained with safranin O/fast green (Carson, 1997) to highlight proteoglycans and glycosaminoglycans (GAGs) content. Microscopical features were evaluated by two veterinary pathologists (RZ, NV) and correlated with the radiographical macro- and micro-architecture. Representative histological sections were scanned with an automated slide scanner (Olympus VS120 Virtual Slide Microscope system, VS120/cellSens, Olympus, Central Valley, Pennsylvania, USA). Scanned digital images were examined using OlyVIA 2.9 Viewer software (Olympus) and captured with ShareX software (GitHub, San Francisco, California, USA).

Results

Cone-beam Computed Tomography

In all five affected cats, CBCT confirmed the clinical diagnosis of TMJ ankylosis. Consistent with the clinical presentation of the immobilized jaw, TMJ ankylosis was severe and bilateral (Fig. 1). Bilateral periosteal bone formation at the condylar processes of the mandible and the temporal portion of the TMJ was observed in three cats. All ankylosed TMJs exhibited mild to severe narrowing of the joint space and altered joint conformation with irregular cortical bone contours. Distorted joint congruity was analogous to a ‘meshed-gear’ shape with either extreme joint space narrowing or focal areas of complete loss of joint space consistent with osseous bridging across the articular surfaces. In addition, the coronoid processes were elongated and curved caudally and had a prominent dorsal bend. Other mandibular changes featured in two cats included shortening of the mandibles. Facial asymmetry was most prominent in one cat, but variably noted in all cases. In contrast, the TMJs of the control cats had a normal joint contour with no signs of bone ankylosis or degenerative changes (Fig. 1).

Analysis of Normal Joints by Micro-computed Tomography and Histology

The four healthy TMJs obtained from the cadavers had no gross, radiographical or microscopical abnormalities. On μCT, the joint space was outlined with smoothly contoured, well-defined subchondral bone in the condylar process of the mandibles and the mandibular fossae (Fig. 2). Well-defined medullary trabecular bone was consistently oriented perpendicular to the articular surfaces and was denser in the mandibular condylar processes than in the temporal bone. Consistently thick subchondral bone had regularly anastomosing medullary trabeculae.

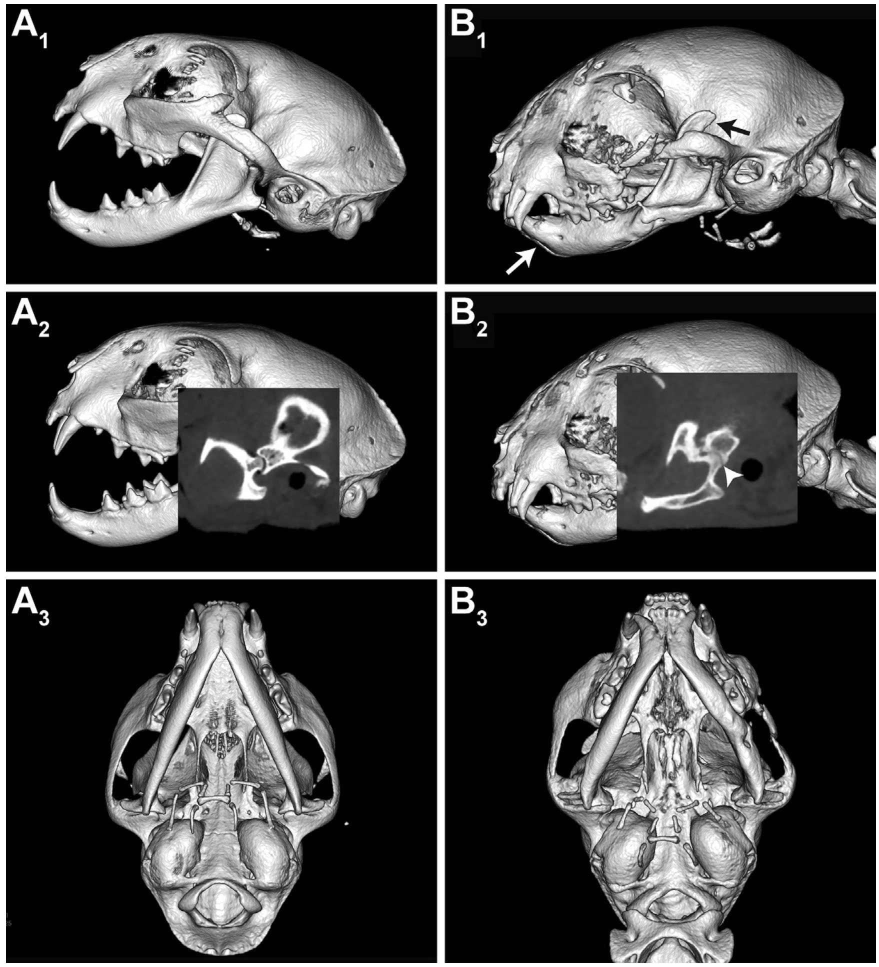

Fig. 1. Three-dimensional images of CBCT of the skulls of a healthy cat (A1, 2 and 3) and a cat affected by bilateral TMJ ankylosis (B1, 2 and 3). All ankylosed TMJs show narrowing of the joint space and altered joint conformation (white arrowhead, B2). Note that the coronoid processes are elongated and curved caudally (black arrow, B1). Relative mandibular brachygnathia is also present in the affected cat (white arrow, B1).

Histologically, a thin cartilaginous layer with patchy GAGs staining (Figs. 3 and 5) interlaced with compact fibrous articular surface and the subchondral bone in the mandibular condylar processes and the mandibular fossa. The medullary trabeculae and cortices were composed of mature, lamellar bone lined with discrete bone lining cells. A medullary trabecular network was denser in the condylar process than in the articulating temporal bone. Only the histological examination provided soft tissue details. The TMJ articular discs were composed of compact fibrous tissue, rarely interrupted with thin vessels and adipocytes at the capsular attachment (Fig. 3). A thin, 1 to 2 cell-thick synovium lined the fibrous joint capsule and approximately 300 μm of the dorsal and ventral aspect of the TMJ disc segment at the capsular attachment. Regularly spaced vascular channels interrupted the subchondral bone. Intertrabecular medullary spaces were filled with adipose tissue intermixed with sparse haemopoietic cells.

Analysis of Affected Joints by Micro-computed Tomography and Histology

All 10 affected joints exhibited intra- and extra-articular features of ankylosis in μCT and histology. The severity of the microscopical degenerative TMJ changes matched the radiographical abnormalities.

The μCT and microscopical findings were complementary and are described together. Profound bone changes were noted. In general, all of the elements of TMJ anatomy such as the orientation of articulating bones, alteration in the osseous components, joint spaces and congruity were disrupted (Fig. 4). The articular margins of the mandibular fossa in the temporal bone and the mandibular condylar processes were poorly defined and irregularly contoured

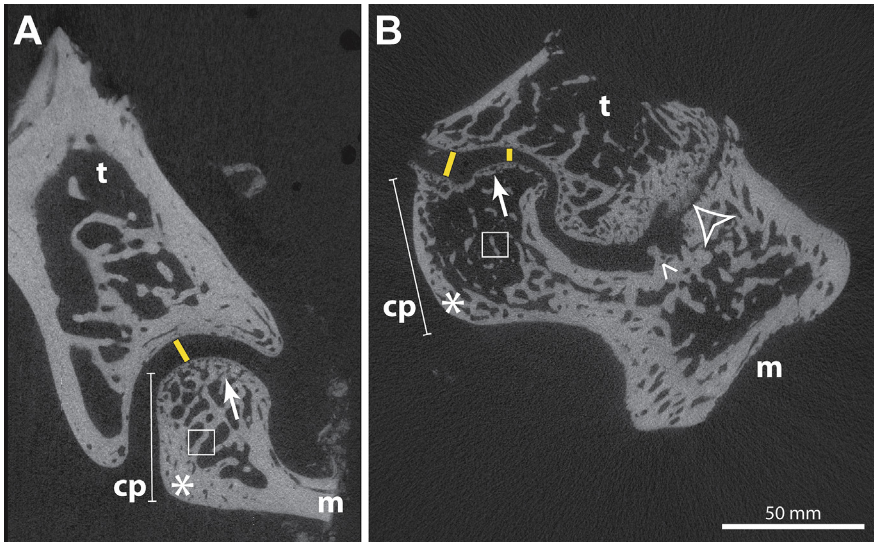

Fig. 2. μCT features of a healthy temporomandibular joint (TMJ) of a domestic cat (A) are compared with the ankylosed TMJ (B) in parasagittal sections. (A) In a healthy joint, the temporal bone (t) and condylar process (cp) assume a hinge-like joint configuration. The joint space (yellow bar) has a consistent width throughout. The trabecular bone of the condylar process (white square) is well defined. (B) The anatomy of the articulating temporal (t) bone and condylar process (cp) of the mandible (m) is markedly altered in the ankylosed TMJ. The hinge-like joint configuration is lost due to poorly delineated joint margins, undulating articulation with variable and narrowed joint space (yellow bars show joint space variation), and extra-articular focal and broad osseous bridging (chevron arrow and empty arrowhead). Subchondral plate (thin white arrow) thinning, and sclerosis are also observed. Loss of bone tissue presents with porosity (osteopaenia) of the cortical bone (asterisk) in the condylar process of the mandible. Medullary trabecular bone (white square) numbers, thickness, contours, orientation and spacing vary in affected TMJs. cp, mandibular condylar process; t, temporal bone; m, mandible.

(Figs. 2 and 4). Intra- and extracapsular osseous bridges, fissures and corresponding invaginations with conforming protrusions were noted in serial μCT images and histology (Figs. 2 and 4).

Subchondral, cortical and medullary bone varied in thickness and density, ranging from sclerotic to osteopaenic compared with the controls. Mineralized cartilage was exposed at the articular surface, where the fibrous layer was eroded. Areas of sclerosis contained increased numbers of osteons and haphazardly organized bone lamellae with rare regions of woven bone. In contrast, the osteopaenic regions were characterized by frequent resorption pits lined with osteoclasts (Fig. 4). Active osteoblasts commonly outlined the bone surfaces in affected TMJs compared with quiescent, flat, bone lining cells in control joints. Overall, increased osteoclastic and osteoblastic activity with prominent areas of resorption and new bone formation coincided with irregular cortical contours, as well as radiolucencies. μCT and histology highlighted irregular distribution and variable thickness of the medullary trabeculae in affected joints. Islands and plates of cartilage embedded in thickened cortical bone, and callus formations, were noted in one case where the abundant, periarticular bone formation was also noted radiographically. With regards to soft tissues, disruption and loss of the compact fibrous articular layer at the joint surfaces, as well as thinning, necrosis of fibrocartilage, loss/rupture, degeneration and peripheral retraction of the disc fibres, characterized the degenerative joint changes (Fig. 4). Histologically, the fibrous and fibro-osseous ankylosis also contained segments of cartilaginous components. The cartilaginous components were contiguous with the plane of the joint space. Prominent vascular profiles were also observed within the fibrous components. Intertrabecular medullary spaces were filled with adipose and plump fibrous stromal tissues, intermixed with sparse haemopoietic cells. Synovial hyperplasia or inflammation, joint effusion, haemorrhage or pannus formation were not observed in any of the examined sections from affected TMJs.

Discussion

To the authors' knowledge, this is the first comprehensive characterization of the intra- and extra-articular features of TMJ ankylosis in cats using CBCT, μCT and histology. Firstly, we noted features of bilateral true and pseudoankylosis of the TMJs in all five affected cats. Secondly, the intra-articular changes of ankylosed TMJs included narrowing of the joint space, degenerative changes of the articular

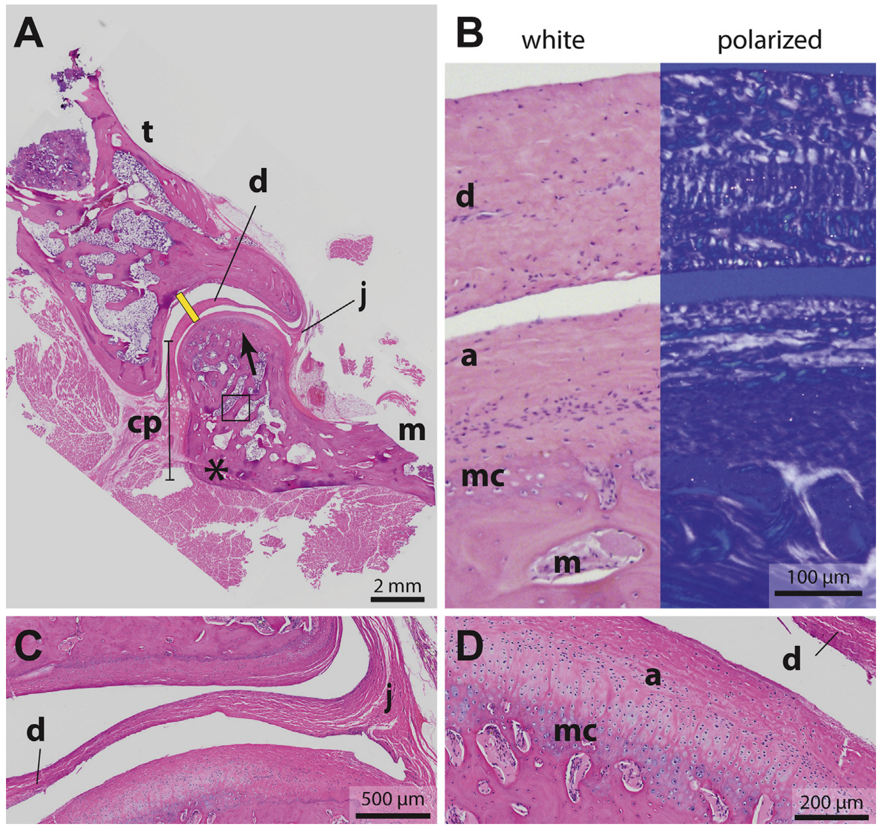

Fig. 3. Microscopical features of a healthy TMJ of a cat in a parasagittal section are demonstrated in the panel of micrographs at different magnifications. (A) Low-power micrograph of the entire TMJ illustrates the concave mandibular fossa of the squamous part of the temporal bone (t) articulating with the convex condylar process (cp) of the mandible (m). At this level of section, the articulation forms a hinge-like joint configuration. The joint is separated into non-communicating dorsal and ventral compartments by the fibrous articular disc (d) that interdigitates with the joint capsule (j). The joint space (yellow bar) and subchondral plate (thin black arrow) are well defined. Cortical and medullary trabecular bone are composed of dense lamellar bone. (B) Articular surface of the condylar process, subchondral bone, medullary cavity and the disc are shown under white and polarized (blue-tinged image) light in the high-power view of the condylar process. Polarized light highlights thick, cross-hatched bundles of the collagen lamellae in the disc (d), the dense, mostly parallel to the surface, articular fibrous layer (a), and the collagen bundles separated by chondrocyte lacunae in the mineralized cartilage (mc) layer. Trabecular bone in the medullary cavity has the dense collagen lamellae with sparse osteocyte lacunae. (C) In this section, the disc (d) seamlessly integrates with the joint capsule (j). At the joint margin, a subtle synovial layer lines the intra-articualar surface of the joint capsule. (D) High-power view of the articular surface of the condylar process is shown. Pale blue chondroid matrix surrounds chondrocytes in the mineralized cartilage layer (mc) defined by tidemark and chondroid cells within the articular layer. Fibrous bands at the articular surface interdigitate with the subjacent cartilage. Clear spaces within the joint mark the location of the joint fluid normally free of cells and debris. Some sectioning artifact is present as intra-articular debris in (B). cp, condylar process; t, temporal bone; m, mandible; d, disc; j, joint capsule; mc, mineralized cartilage. HE.

surfaces and the disc, as well as alteration of the subchondral and cortical bone with osseous bridging in some cases. Finally, the extra-articular changes of ankylosed TMJs included formation of complex, periarticular osseous and soft tissue bridges with the zygomatic arch, the coronoid process and adjacent temporal bone. Taken together, these changes contributed to TMJ fusion, immobilization and altered joint shape that resulted clinically in complete inability to open the mouth.

In this cohort of cats, two cats had a history of trauma while the other three were adopted, and history of trauma remains elusive. Although other aetiologies can lead to ankylosis, maxillofacial trauma is considered the most common cause (Meomartino *et al.*, 1999; Maas and Theyse, 2007; Allori *et al.*, 2010; Cetinkaya, 2012; Anyanechi, 2015; Kaur *et al.*, 2015). Comparatively, in man, trauma and infection are the most common aetiological factors resulting in ankylosis (Kaur *et al.*, 2015; Ma *et al.*, 2015). Inflammatory conditions such as infectious or autoimmune arthritis, irradiation, prior surgery and genetic factors are also reported in people with TMJ ankylosis (Kaur *et al.*, 2015; Cheong *et al.*, 2016). In dogs, craniomandibular osteopathy may result in TMJ ankylosis (Strøm *et al.*, 2016). TMJ ankylosis

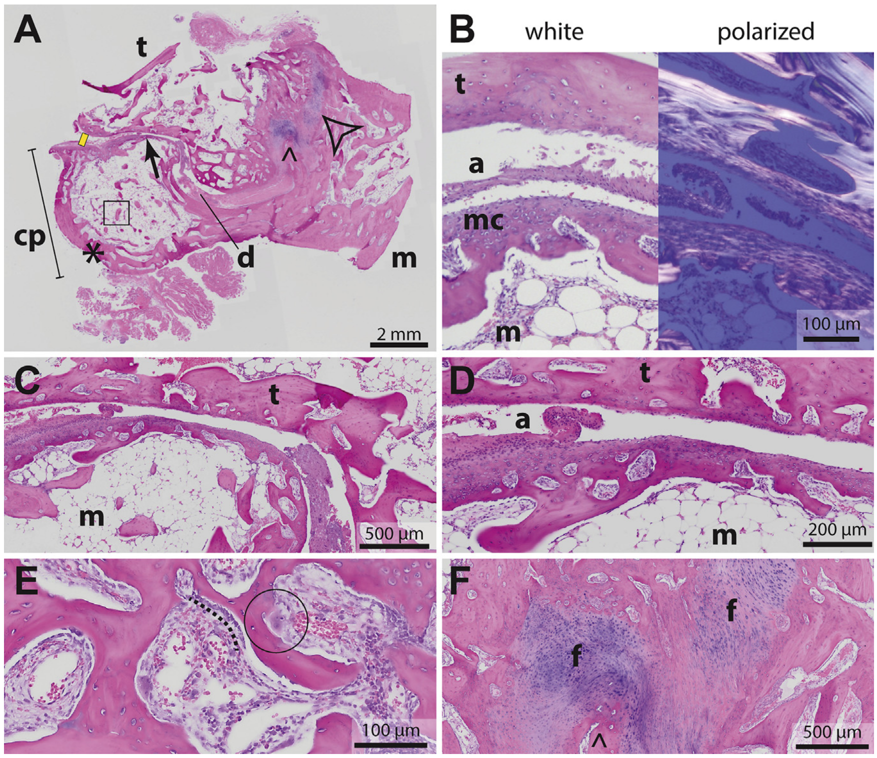

Fig. 4. Microscopical alteration in the soft and osseous components of the ankylosed TMJs are presented in this panel of micrographs. The alterations correspond with the radiographical changes identified with CBCT and µCT. (A) The overall anatomy of the ankylosed TMJ is markedly altered. The hinge-like joint configuration seen in a healthy TMJ (Fig. 2A) is lost due to poorly delineated joint margins, undulating articulation with variable and narrowed joint space (yellow bar), and extra-articular focal and broad osseous bridging (black chevron arrow and empty arrowhead). Loss of bone tissue presents as porosity in the cortical bone (asterisk) and regional thinning of the subchondral plate (thin black arrow). Medullary trabecular bone numbers, thickness, orientation and spacing vary in affected TMJs (black square). The torn fragments of the disc (d) material are displaced. (B) High-power magnification of the articular surface of the condylar process of the mandible (m) and a closely opposed segment of the temporal bone (t) is shown under white and polarized (blue-tinged image) light. Note the absence of the disc. Other degenerative joint changes include thinning, fragmentation, enfolding and erosion of the articular soft tissues (a). Polarized light highlights the articular surface reduced to a thin plate of mineralized cartilage (mc) with the paucity of subjacent medullary trabeculae. (C) In this higher-power view of the ankylosed TMJ, degenerate, amorphous disc (d) material is displaced and the joint margin and joint capsule cannot be defined (should be 500 µm). (D) Note the fibrous articular cartilage portion is detached and folded (a). (E) High-magnification image of the trabecular bone of the condylar process. Note the osteoclasts (encircled) and osteoblasts (dotted line) frequently line the bone surfaces. (F) Area of ankylosis highlighted with an empty arrowhead in (A) is shown under higher magnification. Ankylosing tissue contains osseous projections (chevron arrow) embedded within fibrous and fibrocartilaginous tissues (f). Joint effusion, inflammation, haemorrhage or synovial hyperplasia are not noted in the ankylosed TMJ. cp, condylar process; t, temporal bone; m, mandible; d, disc; f, fibrocartilaginous tissue.

may also result from complication of neoplastic processes (Schwarz *et al.*, 2002; Gatineau *et al.*, 2008). The latter justifies the submission of resected fragments for histopathological evaluation. Finally, congenital ankylosis is considered uncommon. Taken together, given the young age of all the cats in this study and the findings that two of the cats had radiological evidence of trauma and the rest of the cats had an unknown history, it is plausible that traumatic events preceded the bilateral TMJ ankylosis.

The development of TMJ ankylosis in man is poorly understood. This arises from the rarity of the condition and the prolonged period that usually elapses between the initial trauma and ankylosis (Neville *et al.*, 2002; Anyanechi, 2015). Few of the prevalent theories for TMJ ankylosis include the severity of TMJ trauma and displacement of the TMJ disc and destruction of the articular soft tissues. Additionally, occurrence of intra- or extracapsular haemorrhage has also been incriminated (Yan *et al.*, 2014b, 2014c). In the present study, there was no evidence of haemosiderin-laden macrophage infiltration to support historical presence of intra- or extra-articular haemorrhage, likely due to the time lapse between the insult and the development of ankylosis. Studies of induced TMJ ankylosis in animal models indicate that discectomy and injury to both articular

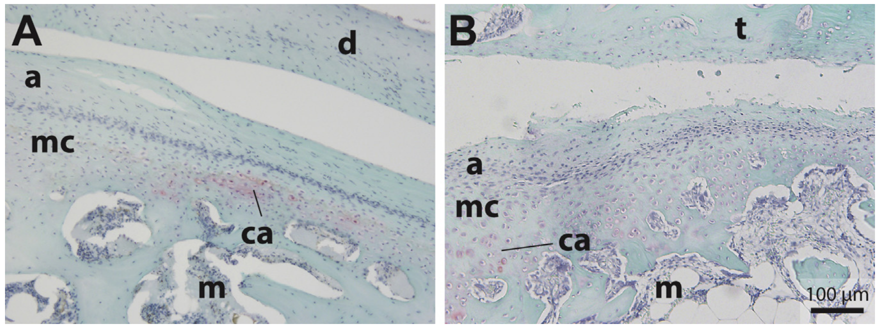

Fig. 5. Microscopical details of the articular surface of the condylar processes (cp) in parasagittal sections of a normal (A) and an ankylosed (B) TMJ. (A) Note the minimal amount of glycosaminoglycan in the cartilaginous (ca) layer in the normal joint. The fibrous layer of the articular surface or the disc lack histochemically detectable glycosaminoglycan. (B) The glycosaminoglycan in the chondroid layers appears depleted (ca) in the ankylosed TMJ. The fibrous superficial layer (a) is disrupted and fibrillated, and the disc is absent. The mandibular fossa of the temporal bone (t) is visible due to narrowed joint space. t, temporal bone; m, mandibular bone; d, disc; ca, cartilaginous layer. Safranin O/fast green stain.

surfaces are the prerequisites for ankylosis (Yan *et al.*, 2014b, 2014c). Restricted jaw movement, however, is not the determining factor, but a promoting condition for the latter. In agreement with these reports, the affected TMJs in the present study exhibited evidence of disc and articular soft tissue degeneration. However, it is unclear whether the degenerative changes observed here were a result of the profound immobility of the joint or a result of the historical trauma. Regardless, these theories suggest that trauma with sufficient destruction of soft tissue is necessary for TMJ ankylosis development.

Microscopical examination of the ankylosed TMJs supported and agreed with the radiographical findings and provided in-depth characterization of the changes in and around the joints. Degenerative changes in the soft tissues of the TMJs were comprised of thinning and necrosis of the articular fibrocartilage and articular disc, and fraying of the articular surfaces.

Degenerative changes involving osseous components included subchondral sclerosis of the mandibular condyles and mandibular fossa and cortical expansion of the mandibular condylar processes with concurrent evidence of osteopaenia in the same articulating components. Cumulatively these changes are indicative of osseous modelling leading to maladaptive healing. The microscopical evidence of intra-articular osseous or fibrous bridging across articular surfaces is in agreement with the CBCT findings and indicates that there was evidence of both intra- and extra-articular ankylosis. These findings further support the utilization of CBCT as an ultimate tool for confirming the clinical diagnosis of TMJ ankylosis and histology for ruling out neoplastic causes (Petrikowski, 2016; Arzi, 2020; Cissell *et al.*, 2020).

The biomechanical aspects of TMJ ankylosis are intriguing. For instance, the restriction of TMJ movement is most typical in the closed mouth position (Strøm *et al.*, 2016; Arzi, 2020). As mentioned previously, the muscles responsible for closing the mouth are more abundant and more powerful than the muscles responsible for the opposite motion (Evans and de Lahunta, 2013). As such, it is plausible that a closed mouth conformation is an outcome of muscle spasm associated with either the initial trauma or the development of TMJ ankylosis. Importantly, the presence of bone sclerosis with concurrent osteopaenia indicates altered and inappropriate loading of the articulating bones. Our findings are in agreement with those in man, where concurrent bone radiolucency and excessive bone density were detected (Yan *et al.*, 2014c).

Some studies suggest that fibrous ankylosis is an earlier stage preceding bony ankylosis (Miller *et al.*, 1975). However, later studies determined that fibro-osseous ankylosis and not the fibrous ankylosis is the early form of bony ankylosis (Yan *et al.*, 2013). Conclusions combined from multiple animal studies with induced TMJ ankylosis indicate that relatively mild trauma results in fibrous ankylosis, while more severe trauma results in bony ankylosis (Yan *et al.*, 2013).

Additionally, and in support of this conclusion, elevated expression of the bone morphogenetic protein (BMP) and Wnt-signalling (a pathway that regulates important aspects of cell fate, migration, polarity, patterning and organogenesis during embryonic development) was demonstrated during the development of bony ankylosis (Yan *et al.*, 2014a, 2014b). Although evaluation of BMP expression was not performed in our cases, future studies in animals with spontaneously occurring TMJ trauma may inform the human medical field. The tissue type present in ankylosis is clinically relevant, because patients with fibrous ankylosis should experience better jaw mobility than patients with bony ankylosis. Therefore, a study of factors that can direct the progression of ankylosis towards a fibrous type would assist efforts aimed at ameliorating the severity of the condition.

In summary, the present study demonstrates that TMJ ankylosis in cats exhibits features of fibro-osseous change resulting in complete inability to open the mouth. The extra- and intra-articular osseous bridging and degenerative joint changes portray maladaptive healing responses and likely represent true ankylosis. Diagnostic imaging via CBCT was crucial for confirmation of the clinical diagnosis, definition and high resolution of the architecture of the TMJ fusions. The understanding that fibro-osseous changes occurred at both the condylar process of the mandibles and the mandibular fossa of the squamous temporal bone have clinical importance for surgical planning, as both components of the ankylosis should be removed in order to enable mouth opening. Further studies in companion animals with spontaneously occurring TMJ may provide a suitable model for further studies in man and other species.

Acknowledgments

Financial support for this work was provided by the Foundation for Veterinary Dentistry research grant. The author NV was supported by NIH grants T32–OD011147 and KL2–TR001859. The content is solely the responsibility of the authors and does not necessarily represent the official views of the National Institute for Health. The authors thank Dr. C. A. Toupadakis Skouritakis for assistance with the figures.

References

Allori AC, Chang CC, Farina R, Grayson BH, Warren SM *et al*. (2010) Current concepts in pediatric temporomandibular joint disorders: Part 1. Etiology, epidemiology, and classification. *Plastic and Reconstructive Surgery*, **126**, 1263–1275.

Anyanechi CE (2015) Temporomandibular joint ankylosis caused by condylar fractures: a retrospective analysis of cases at an urban teaching hospital in Nigeria. *Internatioanl Journal of Oral and Maxillofacial Surgegy*, **44**, 1027–1033.

Arzi B (2020) Temporomandibular joint ankylosis and pseudoankylosis. In: *Oral and Maxillofacial Surgery in Dogs and Cats*, FJM Verstraete, MJ Lommer, B Arzi, Eds., Elsevier, St. Louis, pp. 377–382.

Arzi B, Cissell DD, Verstraete FJM, Kass PH, DuRaine GD *et al*. (2013) Computed tomographic findings in dogs and cats with temporomandibular joint disorders: 58 cases (2006–2011). *Journal of the American Veterinary Medical Association*, **242**, 69–75.

Arzi B, Staszyk C (2019) The temporomandibular joint through the lens of comparative anatomy. In: *Contemporary Management of Temporomandibular Disorders*, S Connelly, G Tartaglia, R Silva, Eds., Springer Nature, Basel, pp. 41–50.

Arzi B, Verstraete FJM, Garcia TC, Lee M, Kim SE *et al*. (2019) Kinematic analysis of mandibular motion before and after mandibulectomy and mandibular reconstruction in dogs. *American Journal of Veterinary Research*, **80**, 637–645.

Bar-Am Y, Pollard RE, Kass PH, Verstraete FJM (2008) The diagnostic yield of conventional radiographs and computed tomography in dogs and cats with maxillofacial trauma. *Veterinary Surgery*, **37**, 294–299.

Carson FL (1997) *Histotechnology: A Self-Instructional Text*. ASCP Press, Chicago, pp. 89–95.

Cetinkaya MA (2012) Temporomandibular joint injuries and ankylosis in the cat. *Veterinary and Comparative Orthopaedics and Traumatology*, **25**, 366–374.

Cheong RC, Kassam K, Eccles S, Hensher R (2016) Congenital temporomandibular joint ankylosis: case report and literature review. *Case Reports in Otolaryngology*, **2016** 5802359.

Cissell DD, Hatcher D, Arzi B, Verstraete FJM (2020) Diagnostic imaging in oral and maxillofacial surgery. In: *Oral and Maxillofacial Surgery in Dogs and Cats*, FJM Verstraete, MJ Lommer, B Arzi, Eds., Elsevier, St. Louis, pp. 56–64.

Evans HE, de Lahunta A (2013) Ligaments and joints of the skull. In: *Miller's Anatomy of the Dog*, HE Evans, A de Lahunta, Eds., Elsevier Saunders, St. Louis, pp. 161–162.

Gatineau M, El-Warrak AO, Marretta SM, Kamiya D, Moreau M (2008) Locked jaw syndrome in dogs and cats: 37 cases (1998–2005). *Journal of Veterinary Dentistry*, **25**, 16–22.

Hennet PR, Harvey CE (1992) Craniofacial development and growth in the dog. *Journal of Veterinary Dentistry*, **9**, 11–18.

Kaur T, Krishnan G, Sharma A (2015) Factors influencing treatment plan and post operative compliance in TMJ ankylosis patients: a retrospective analysis of long term post surgical evaluation. *Journal of Maxillofacial and Oral Surgery*, **14**, 17–23.

Lin AW, Vapniarsky N, Cissell DD, Verstraete FJM, Lin CH *et al*. (2018) The temporomandibular joint of the domestic dog (*Canis lupus familiaris*) in health and disease. *Journal of Comparative Pathology*, **161**, 55–67.

Ma J, Liang L, Jiang H, Gu B (2015) Gap arthroplasty versus interpositional arthroplasty for temporomandibular joint ankylosis: a meta-analysis. *PLoS One*, **10** e0127652.

Maas CP, Theyse LF (2007) Temporomandibular joint ankylosis in cats and dogs. A report of 10 cases. *Veterinary* *and Comparative Orthopaedics and Traumatology*, **20**, 192–197.

Meomartino L, Fatone G, Brunetti A, Lamagna F, Potena A (1999) Temporomandibular ankylosis in the cat: a review of seven cases. *Journal of Small Animal Practice*, **40**, 7–10.

Miller GA, Page HL Jr., Griffith CR (1975) Temporomandibular joint ankylosis: review of the literature and report of two cases of bilateral involvement. *Journal of Oral Surgery*, **33**, 792–803.

Movahed R, Mercuri LG (2015) Management of temporomandibular joint ankylosis. *Oral and Maxillofacial Surgery Clinics of North America*, **27**, 27–35.

Neville BW, Damm DD, Allen CM (2002) Facial pain and neuromuscular diseases. In: *Oral and Maxillofacial Pathology*, BW Neville, DD Damm, CM Allen, Eds., WB Saunders, Philadelphia, pp. 741–759.

Nickel R, Schummer A, Seiferle E (1986) *The Anatomy of the Domestic Animals*. Verlag Paul Parey Press, Berlin, p. 111.

Petrikowski CG (2016) Bone ankylosis. In: *Specialty Imaging Temporomandibular Joint*, D Tamimi, D Hatcher, Eds., Elsevier, Philadelphia, pp. 524–525.

Schwarz T, Weller R, Dickie AM, Konar M, Sullivan M (2002) Imaging of the canine and feline temporomandibular joint: a review. *Veterinary Radiology & Ultrasound*, **43**, 85–97.

Sidebottom AJ, Salha R (2013) Management of the temporomandibular joint in rheumatoid disorders. *British Journal of Oral and Maxillofacial Surgery*, **51**, 191–198.

Strøm PC, Arzi B, Cissell DD, Verstraete FJM (2016) Ankylosis and pseudoankylosis of the temporomandibular joint in 10 dogs (1993–2015). *Veterinary and Comparative Orthopaedics and Traumatology*, **29**, 409–415.

Yan YB, Li JM, Xiao E, An JG, Gan YH *et al*. (2014a) A pilot trial on the molecular pathophysiology of traumatic temporomandibular joint bony ankylosis in a sheep model. Part I: expression of Wnt signaling. *Journal of Craniomaxillofacial Surgery*, **42**, e15–e22.

Yan YB, Li JM, Xiao E, An JG, Gan YH *et al*. (2014b) A pilot trial on the molecular pathophysiology of traumatic temporomandibular joint bony ankylosis in a sheep model. Part II: the differential gene expression among fibrous ankylosis, bony ankylosis and condylar fracture. *Journal of Craniomaxillofacial Surgery*, **42**, e23–e28.

Yan YB, Liang SX, Shen J, Zhang JC, Zhang Y (2014c) Current concepts in the pathogenesis of traumatic temporomandibular joint ankylosis. *Head & Face Medicine*, **10**, 35.

Yan YB, Zhang Y, Gan YH, An JG, Li JM *et al*. (2013) Surgical induction of TMJ bony ankylosis in growing sheep and the role of injury severity of the glenoid fossa on the development of bony ankylosis. *Journal of Craniomaxillofacial Surgery*, **41**, 476–486.

Yuan F, Sui H, Li Z, Yang H, Lu P *et al*. (2015) A method of three-dimensional recording of mandibular movement based on two-dimensional image feature extraction. *PLoS One*, **10** e0137507.

[*Received, November 5th, 2019*
Accepted, December 21st, 2019]